

PARTICLE SIZE AND FILLER-MATRIX ADHESION EFFECTS ON DYNAMIC FRACTURE OF GLASS-FILLED EPOXY COMPOSITES

Hareesh Tippur and Rajesh Kitey
Department of Mechanical Engineering,
Auburn University, Alabama 36849, USA

ABSTRACT

Role of particle size and filler-matrix adhesion strength on dynamic fracture behavior of glass-filled epoxy is studied. Spherical particles of size ranging from $7\ \mu\text{m}$ to $200\ \mu\text{m}$ are used to reinforce epoxy matrix at a constant volume fraction (10%) and two different filler-matrix strengths, weak and strong. Filler particle size affects fracture toughness significantly when particles are weakly bonded to the matrix. Additionally, a particle size of $35\ \mu\text{m}$ is seen to enhance the fracture toughness the most when compared to both smaller and larger uncoated particles. An inverse relationship seems to exist between steady state fracture toughness and crack velocity for different particle sizes. Unlike weakly bonded fillers, the size effect essentially vanishes when fillers are strongly bonded to the matrix.

1 INTRODUCTION

The properties of the constituent phases, filler volume fraction, filler particle size and shape, and filler-matrix interfacial strength significantly influence these overall properties of particulate composites in general and failure properties such as tensile strength and fracture toughness in particular. Previous experimental attempts[1-5] and modeling efforts[6-9] towards quantifying these have generally been made under quasi-static loading conditions and dynamic responses are largely unknown at the moment. In this paper, particle size and filler-matrix adhesion effect on fracture behavior of glass-filled epoxy have been investigated under impact loading conditions. Crack initiation and crack growth phenomena along with crack tip deformations have been measured using high-speed imaging and optical interferometry.

2 MATERIAL PREPARATION AND CHARACTERIZATION

Soda-lime glass spheres (10% volume fraction, V_f) are chosen to prepare glass-filled epoxy specimens for the study. Solid glass spheres of mean diameters $7\ \mu\text{m}$, $11\ \mu\text{m}$, $35\ \mu\text{m}$, $71\ \mu\text{m}$ and $203\ \mu\text{m}$ have been used to study particle size effect. To study filler-matrix adhesion effect, weak and strong filler-matrix interfaces has been created by using uncoated and silane coated particles of the above mentioned sizes. It should be noted, however, that particle sizes $11\ \mu\text{m}$, $35\ \mu\text{m}$ and $203\ \mu\text{m}$ are the only ones available commercially for the silane treated case.

Longitudinal and shear wave speeds (C_l and C_s) are measured by *pulse-echo method*. Dynamic elastic Modulus $E(= 4.9 \pm 0.05\text{GPa})$ and Poisson's ratio $\nu(= 0.365)$ are

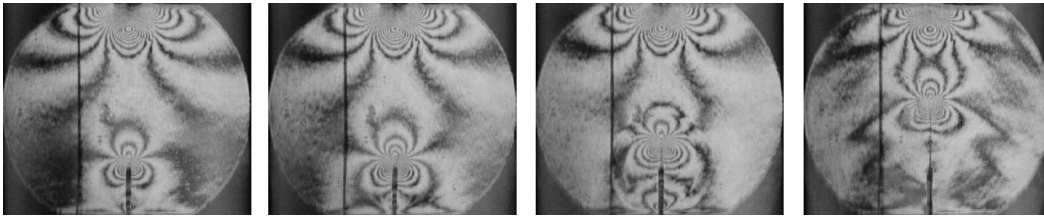


Figure 1: Fringe pattern representing contours of $\partial w/\partial x$ for $11\ \mu\text{m}$ weakly bonded particles at various time instants, $80\ \mu\text{sec}$, $100\ \mu\text{sec}$, $120\ \mu\text{sec}$ and $140\ \mu\text{sec}$

calculated using the wave speeds and the mass density of the composite. Measurements show that particle size or surface treatment do not affect elastic properties in any significant way. The elastic wave speeds are in the range of $C_l = 2560 \pm 25\text{m/sec}$, $C_s = 1170 \pm 10\text{m/sec}$ and density $\rho = 1285 \pm 10\text{kg/m}^3$. Cast sheets are machined into test specimens of dimensions $152\ \text{mm} \times 42\ \text{mm} \times 8\ \text{mm}$. Subsequently, the surface is made optically flat and specular. An edge notch of length of $10\ \text{mm}$ is cut into the fracture specimens.

3 EXPERIMENTAL DETAILS

The optical method of Coherent Gradient Sensing, CGS[10], in conjunction with high-speed photography, has been used to study crack tip deformations in particle filled composite specimens. The experimental set-up includes an impactor, a pulse laser, CGS interferometer and a continuous access high-speed camera. Edge notched specimens are subjected to symmetric impact loading (vel. $5.3\ \text{m/sec}$) in the free-free beam configuration and crack tip fields are recorded prior to and after crack initiation. The angular deflections of light rays relative to the optical axis are measured as interference fringes. The fringe patterns representing contours of $\partial w/\partial x$ are recorded in this study.

Following impact loading, a crack propagates dynamically at speeds of up to $530\ \text{m/sec}$ in some specimens. A set of four fringes for $11\ \mu\text{m}$ weakly bonded particles are shown as an example in Fig.1. Impact point fringes (at the top of every image) develop and start accumulating as soon as impactor contacts the specimen, while the crack tip fringes start appearing after about $35 - 40\ \mu\text{sec}$ after the initial impact. As the stress waves reach the crack tip, start evolving around the crack tip. These fringes represent contours of $\partial w/\partial x$ where w is out-of-plane displacement. The resolution of the fringes is $\approx 0.015^\circ/\text{fringe}$.

Surface deformations are measured in terms of fringe order N , grating pitch p and grating separation distance Δ . In the present work, the principal direction of the

Mean particle diameter $D(\mu m)$	Maximum crack velocity $v_{max}(m/sec)$	Steady state crack velocity $v_{ss}(m/sec)$	Steady state duration $t_{ss}(\mu sec)$	Crack initiation toughness $K_{Ii}(MPa\sqrt{m})$	Steady state fracture toughness $K_{Iss}(MPa\sqrt{m})$
203*	325	310	55	1.89	1.65
71*	341	300	50	2.19	1.92
35*	382	285	45	2.48	2.31
11*	464	345	35	2.25	1.96
7*	493	370	25	1.97	1.87
epoxy	350	325	45	2.28	1.5
203**	366	312	35	1.79	1.65
35**	428	320	30	1.93	1.77
11**	536	375	15	1.73	1.65

* uncoated particles, ** silane treated particles

Table 1: Crack growth parameters for glass-filled epoxy with weakly and strongly bonded filler ($V_f=0.1$)

gratings is chosen to be along the x -axis. Hence[10],

$$\frac{\partial w}{\partial x} \approx -\frac{\nu B}{2E} \left[\frac{\partial(\sigma_x + \sigma_y)}{\partial x} \right] = \frac{Np}{2\Delta}, \quad N = 0, \pm 1, \pm 2, \pm 3, \dots,$$

where B is the undeformed thickness of the specimen. Considering asymptotic stress field in the vicinity of a steadily propagating mode-I crack, the interferograms have been analyzed. Instantaneous crack length is measured from the images and crack velocities are calculated using central difference method. Interferograms are analyzed using an overdeterministic least-squares analysis to evaluate instantaneous stress intensity factors (SIF) K_I .

4 RESULTS AND DISCUSSIONS

4.1 Particle size effect

Weakly bonded particles: Crack velocity histories for specimens with weakly bonded fillers are shown in Fig.2(a). Only the results for 11 μm , 35 μm and 203 μm sizes are shown in order to avoid data clutter and consistent comparison with strongly bonded fillers to be presented later. In each case crack velocity history shows rapid increase at initiation reaching a maximum value v_{max} , followed by a noticeable drop. Subsequently, crack velocity is oscillatory about an average value identified as steady state velocity, v_{ss} . Some of these observations about crack initiation and growth are quantified in Table 1. The maximum crack velocity following

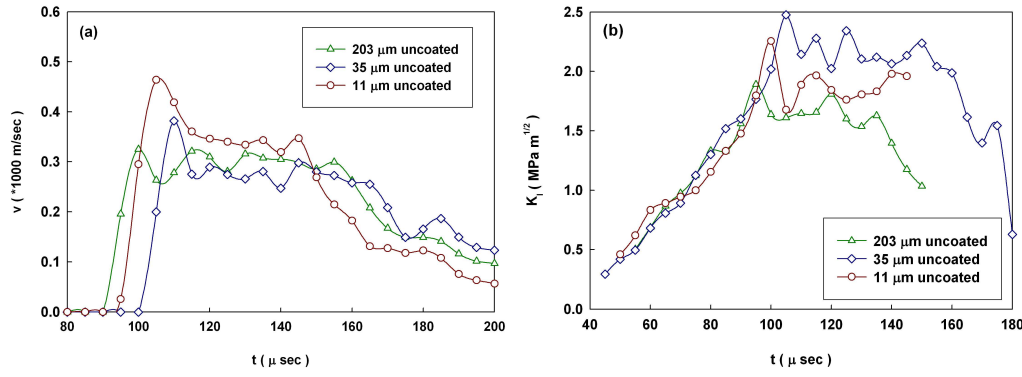


Figure 2: Crack velocity histories (a) and Stress intensity factor histories (b) for different glass-filled epoxy specimens with weakly bonded (uncoated) particles.

crack initiation increases as the particle size decreases. In the current study the maximum velocity ranges between ~ 325 m/sec for the largest particles to ~ 500 m/sec for the smallest. Table 1 shows minimum steady state velocity in case of $35 \mu m$ particles. Further increase or decrease in particle size only results in an increase in steady state velocity.

K_I histories for specimens with weakly bonded particles (same particle sizes as in Fig.2(a), for consistency) of various particle sizes are shown in Fig.2(b). For each

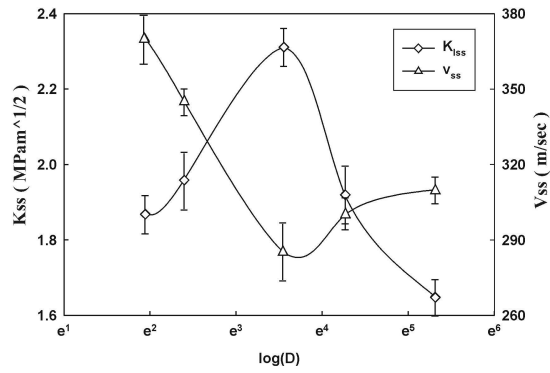


Figure 3: Variation of steady state velocity and fracture toughness with particle size in glass-filled epoxy with weakly bonded fillers.

particle size, SIF monotonically increases until crack initiation. The similarity of pre-initiation SIF histories suggest nearly same crack tip loading rate. This is attributed to similar macroscopic elastic wave characteristics irrespective of particle size and filler-matrix adhesion strength. In each case, crack initiation is followed by a small drop in K_I value and a sustained oscillatory behavior about an average. Notations K_{Ii} and $K_{I_{ss}}$ will henceforth be used for maximum and steady state fracture toughness values, respectively. The K_{Ii} and $K_{I_{ss}}$ values for all weakly bonded particles are also tabulated in Table 1. The

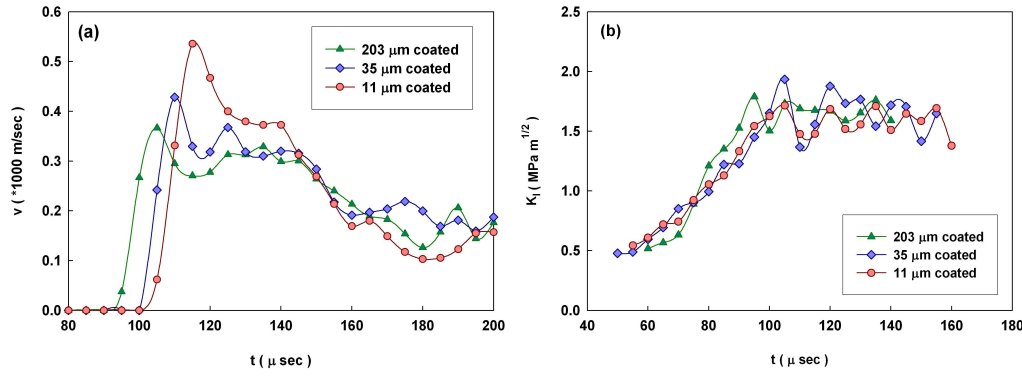


Figure 4: Crack velocity histories (a) and Stress intensity factor histories (b) for different glass-filled epoxy specimens with strongly bonded (silane treated) particles.

$K_{I_{ss}}$ of unfilled epoxy ($\approx 1.5 \pm 0.1 \text{ MPa}\sqrt{\text{m}}$) is considered as a reference for further comparisons. Specimens with $35 \mu\text{m}$ particles show the highest value of $K_{I_{ss}}$, which is approximately 65% higher when compared to the one for unfilled epoxy. With a decrease or an increase in particle sizes relative to $35 \mu\text{m}$ size, $K_{I_{ss}}$ shows decreasing trend. Specimens with $11 \mu\text{m}$ particles show 40% and $7 \mu\text{m}$ particles show 34% higher fracture toughness, respectively, compared to the unfilled epoxy. From Table 1 it can be noticed that both $11 \mu\text{m}$ and $7 \mu\text{m}$ show similar SIF behaviors, with a relatively small difference in $K_{I_{ss}}$ suggesting possible saturation of fracture toughness as particle size decreases. Similar effects have been noticed when particle size is increased beyond $35 \mu\text{m}$. Specimens with $71 \mu\text{m}$ and $203 \mu\text{m}$ particles show approximately 37% and 18% increase in fracture toughness compared to unfilled epoxy, which is successively lower compared to the ones with $35 \mu\text{m}$ particles. The optimum particle size for maximum $K_{I_{ss}}$ also corresponds to the minimum v_{ss} . With a decrease or an increase in particle size relative to the optimum value, monotonic decrease in $K_{I_{ss}}$ is associated with increase in v_{ss} . That is, an inverse relationship between v_{ss} and $K_{I_{ss}}$ exists (see Fig.3). From Table 1 it can also be noticed that K_{I_i} trends are similar to that of $K_{I_{ss}}$. The trends again show optimum particle size to be $35 \mu\text{m}$. Comparison shows that K_{I_i} is higher by 35%, 56%, 77%, 61% and 41% for $203 \mu\text{m}$, $71 \mu\text{m}$, $35 \mu\text{m}$, $11 \mu\text{m}$ and $7 \mu\text{m}$, respectively, compared to the unfilled epoxy.

Strongly bonded particles: To study the particle size effect on fracture behavior in case of silane treated filler, experiments have been performed on three particle sizes, $203 \mu\text{m}$, $35 \mu\text{m}$ and $11 \mu\text{m}$. The selection of particle sizes here is limited due to commercial availability. Figure 4(a) and Fig.4(b) show crack velocity and stress intensity factor histories. From Table 1 it can be noticed that both maximum and

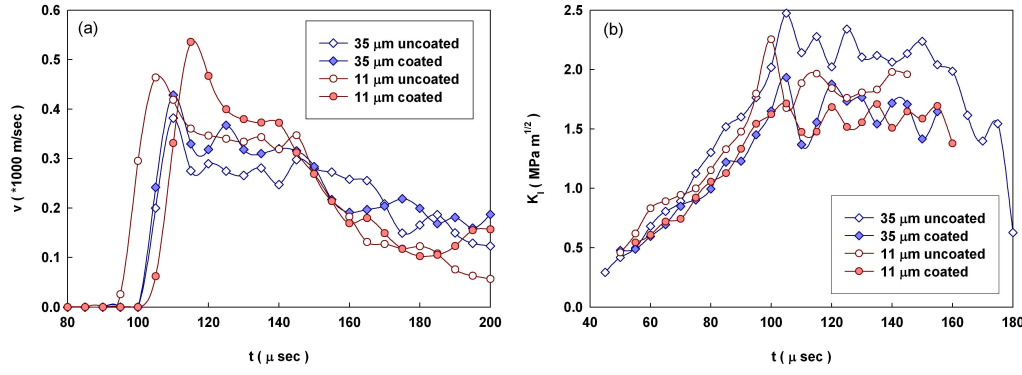


Figure 5: Crack velocity histories (a) and Stress intensity factor histories (b) for different glass-filled epoxy specimens with strongly bonded (silane treated) particles.

steady state velocities increase as particle size decreases. Further, similar to weakly bonded particles, SIF histories in Fig.4(b) show monotonic increase in K_I until crack initiation for all particle sizes. As before, crack initiation is followed by a small drop in K_I and a steadily oscillatory value identified by $K_{I_{ss}}$. Unlike weakly bonded particles, strongly bonded ones do not show significant variation in $K_{I_{ss}}$ as particle size is varied. From SIF histories in Fig.4(b) and Table 1 it is quite clear that $K_{I_{ss}}$ values for various particle sizes are rather close to each other, suggesting only a marginal effect of particle size on fracture toughness in case of strongly bonded particles. Specimens with 35 μ m particles still show slightly higher fracture toughness when compared to the other two particle sizes.

4.2 Filler-matrix adhesion effect

Figure 5(a) isolates filler-matrix adhesion effect on crack velocity. Only the data for particle sizes 35 μ m and 11 μ m have been shown for comparison purposes. From Table 1 it can be concluded that increasing the filler-matrix interface strength increases the v_{max} as well as v_{ss} . Specimens with strongly bonded particles show 12-15% (8 – 10%) higher maximum (steady-state) velocities when compared to the ones with weakly bonded particles for similar particle sizes. For strongly bonded particles v_{ss} values are marginally higher.

The effect of filler-matrix adhesion on fracture toughness can be quantified from Fig.5(b) where 35 μ m and 11 μ m data are compared. Unlike weakly bonded particles, particle size does not affect fracture toughness prominently in case of strongly bonded filler. This suggests that increasing the filler-matrix adhesion affects the fracture toughness somewhat negatively under dynamic loading conditions. From Table 1 it can be noticed that maximum increase in fracture toughness for weakly

bonded filler is for 35 μm particles, which is $\sim 30\%$ higher compared to strongly bonded 35 μm particles. Weakly bonded 11 μm particles show $\sim 18\%$ increase in $K_{I_{ss}}$ values relative to strongly bonded 11 μm particles. Material with 203 μm particles shows negligible effect of filler-matrix adhesion on fracture toughness. Similar trends can be noticed in regards to K_{I_i} , which are 5%, 30% and 30% higher for 203 μm , 35 μm and 11 μm weakly bonded particles as compared to strongly bonded ones.

5 CONCLUSIONS

Dynamic crack initiation and growth in particle filled composites has been studied. Weakly bonded and strongly bonded fillers from 7 μm to 203 μm in sizes are used to prepare test specimens at 10% filler volume fraction. Reflection CGS and high-speed photography are used to measure crack-tip fields. Fracture parameters are evaluated from the interferograms. Particle size and filler-matrix adhesion effects on fracture behavior based on the experiments are summarized in the follows:

(a) Significant particle size effect on fracture toughness has been noticed in weakly bonded particles. There is an optimum particles size (35 μm at 10% V_f in the current study) at which fracture toughness is maximum. Fracture toughness decreases as particle size increases or decreases relative to this particle size.

(b) Maximum crack velocity (v_{max}) increases as particle size decreases for weakly bonded particles. Steady state velocity (v_{ss}) shows an inverse relation with $K_{I_{ss}}$. Minimum v_{ss} corresponds to the optimum particle size of 35 μm and maximum $K_{I_{ss}}$ in this study.

(c) Particle size has little or no effect on fracture toughness (K_{I_i} and $K_{I_{ss}}$) when the filler particles are strongly bonded to the matrix. Hence, increasing filler-matrix adhesion seems to affect the fracture toughness negatively under dynamic loading conditions.

REFERENCES

- (1) Spanoudakis J. and Young R. J., *J. Mater. Sci.* 1984, **19**, 473-486.
- (2) Spanoudakis J. and Young R. J., *J. Mater. Sci.* 1984, **19**, 487-496.
- (3) Moloney A. C., Kausch H. H., Kaiser T. and Beer H. R., *J. Mater. Sci.* 1987, **22**, 381-393.
- (4) Nakamura Y. and Yamaguchi M., *Polymer* 1992, **33(16)**, 3415-3426.
- (5) Nakamura Y., Okabe S. and Iida T., *Polym. Polym. Compos.* 1999, **7(3)**, 177-186.
- (6) Lange F. F., *Phil. Mag.* 1970, **22**, 983-992.
- (7) Faber K. T. and Evans A. G., *Acta Metall.* 1983, **31(4)**, 565-576.
- (8) Faber K. T. and Evans A. G., *Acta Metall.* 1983, **31(4)**, 577-584.
- (9) Evans A. G., *Phil. Mag.* 1972, **26**, 1327-1344.
- (10) Tippur H. V., Krishnaswamy S. and Rosakis A. J., *Int. J. Fract.* 1991, **52**, 91-117.